

# A method to determine collection efficiency of particles by swipe sampling

J R Verkouteren, J L Coleman, R A Fletcher, W J Smith, G A Klouda  
and G Gillen

Surface and Microanalysis Science Division, National Institute of Standards and Technology,  
Gaithersburg, MD 20899, USA

Received 3 July 2008

Published 22 September 2008

Online at [stacks.iop.org/MST/19/115101](http://stacks.iop.org/MST/19/115101)

## Abstract

A methodology was developed to evaluate particle collection efficiencies from swipe sampling of trace residues. Swipe sampling is used for many applications where trace residues must be collected, including the evaluation of radioactive particle contamination and the analysis of explosives and contraband at screening checkpoints using ion mobility spectrometry (IMS). Collection efficiencies were evaluated for micrometer-sized polystyrene latex (PSL) spheres with respect to the particle size and mode of deposition, collection trap, surface type and swiping force. Test surfaces containing particles were prepared under controlled conditions and swiped with a reproducible technique that allows for the evaluation of frictional forces. Collection efficiencies were determined by optical imaging and particle counting. Of the two IMS collection traps studied, the polytetrafluoroethylene (PTFE) trap has significantly lower collection efficiencies. This is likely to be due to a combination of texture and composition. The larger (42  $\mu\text{m}$  diameter) particles are collected more efficiently than the smaller (9  $\mu\text{m}$  diameter) particles. Particles in a matrix similar to latent fingerprints are collected more efficiently than dry particles. Applying greater force during swiping does not greatly improve collection efficiencies. This fact, coupled with the observation that many particles are detached but not collected, implies that improvements in collection efficiency are dependent on improvements in adhesion of the particles to the collection surface, rather than larger forces to detach the particles.

**Keywords:** fluorescence microscopy, particle collection, trace detection, swipe sampling

(Some figures in this article are in colour only in the electronic version)

## 1. Introduction

Physical swiping of surfaces to collect particulate material for analysis is a ubiquitous practice in environmental and forensic sampling. The International Atomic Energy Agency (IAEA) uses swipe sampling for environmental monitoring to verify compliance with nuclear non-proliferation treaties (Donohue 1998). Swipe sampling is used at airports and other security venues to screen personal items for trace levels of explosives that could be indicative of terrorist activity. By 2004, more than 10 000 ion mobility spectrometry (IMS)-based explosive detectors that use swipe sampling had been deployed at airports worldwide (Eiceman and Stone 2004), in addition to the number used by the military and other government agencies. The same detection technology and

swipe sampling is also being used for illicit drug detection in prisons, with additional applications for border security and customs. Common to all swipe sampling is the need for the efficient collection of the sample, as there are generally very small quantities of analyte to harvest (micrograms or less). For example, studies have shown that handling plastic explosives such as C-4 and Semtex H can result in contamination in the form of primary or secondary fingerprints that generally do not contain more than microgram levels of explosives (Gresham *et al* 1994, Hallowell 2001). One of the primary challenges in improving detection efficiency is the effective collection of the sample.

The IAEA employs clean-room wipes as the swipe material, primarily because of the ability to ensure a low background for the analyte of interest (Donohue 1998).

Particles are extracted from the wipe for analysis, and detection efficiency is a function of both collection and extraction efficiencies. In the case of IMS-based trace explosives and drug detection, the sample is analyzed directly from the collection medium. The sampling media are generally referred to as ‘traps’ and are designed to be placed in the front end of the IMS instrument where the particles can be desorbed by proximity to a heater. The development of sample traps by the manufacturers of IMS instruments is generally proprietary, but they are typically a paper or cloth. The traps must withstand typical desorber temperatures of 100 °C–300 °C and should be free of substances that produce an IMS background signal. There may also be some physical requirements for traps, such as rigidity, to meet engineering constraints of the particular instrument. Purchasers of trace explosive/drug detectors would prefer low-cost sample traps to reduce consumable costs.

The development of better sampling media would be facilitated by having test materials and methodologies to evaluate collection efficiency. The need for a standardized method to test collection efficiency is especially acute for IMS-based trace explosive/drug detectors, given the expanding deployment and rapid development of the equipment. This is the application that we focus on in this work. In addition to the needs of technology development, practitioners should have information about how to improve the swiping process, including how hard to swipe and the best surfaces to select. To our knowledge, there are currently no accepted test methods that can be used to measure collection efficiency by swipe sampling. A limited number of studies have been reported on swiping efficiency, specifically for nuclear materials (Jung *et al* 2001) and contraband drugs (Patrick and Poziomek 1997), but these have not attempted to provide a comprehensive evaluation of the factors involved in swiping. These factors include the particle size and composition of the target analyte, the texture and composition of the surface and trap, the force and speed of swiping, and environmental factors that can affect adhesion and removal. This study is the first step in establishing such a method. We use a purely experimental approach to determine swiping collection efficiency, but design the experiment in such a way to provide a framework for future modeling and prediction.

### 1.1. Theory

Swipe sampling involves the removal of particles adhered to a surface with the application of normal and frictional forces, resulting in a collection of the particles on the contacting surface. Much attention has been paid to the removal of small particles, particularly with regard to semiconductor processing, and fundamental studies of the forces involved are available in the literature (e.g. Ranade 1987, Visser 1995, Rimai and DeMejo 1996). The predominant forces affecting particle adhesion and removal are shown in figure 1, for the idealized case of a sphere contacting a flat plane in an air environment. This treatment is adapted from the modeling of brush scrubber cleaning of wafer surfaces (Burdick *et al* 2001, Xu *et al* 2004, 2005), which uses similar physical methods to

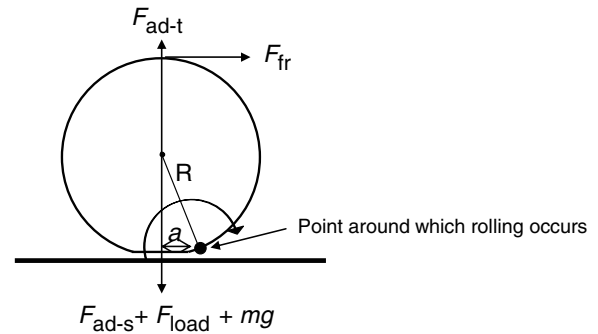


**Figure 1.** Force diagram for sphere adhesion and removal from a flat plane using swipe sampling.

remove particles from surfaces. The adhesive forces between the particle and the surface ( $F_{ad-s}$ ) include the van der Waals force, the electrostatic force and the capillary force. Additional forces include the load ( $F_{load}$ ) exerted by the trap (the brush in the case of brush scrubber cleaning) and the gravitational force. Adhesive forces induce a deformation in either the sphere or the surface such that there is an extended area of contact of the radius  $a$  between the particle and the surface. The removal forces include the adhesive force between the particle and the trap ( $F_{ad-t}$ ), which includes van der Waals, electrostatic and capillary forces and the frictional force ( $F_{fr}$ ) between the particle and the trap. There is an additional hydrodynamic drag force involved in brush scrubber cleaning arising from the use of a lubricant, which is not relevant to dry swiping. It is common to use lubricants for swiping, but not for screening personal objects that cannot be damaged or altered.

Particles are removed primarily by two mechanisms, lifting and rolling. For our purposes, we are interested in lifting, as lifting results in the attachment of the particles to the trap, whereas rolling simply moves particles along the surface. Lifting occurs when the forces attaching the particles to the trap exceed those attaching the particles to the surface:

$$F_{ad-t} > F_{ad-s} + mg. \quad (1)$$

The downward force on the particle,  $F_{load}$ , disappears during vertical lifting. Rolling occurs when the removal moments exceed the adhesion moments:

$$a(F_{ad-s}) + 2R(F_{fr}) > a(F_{ad-s} + F_{load} + mg), \quad (2)$$

where  $R$  is the radius of the particle. A third mechanism for particle removal, sliding, is intermediate between lifting and rolling (Wang 1990) and can be disregarded in a general discussion of removal forces.

The van der Waals forces can be calculated for the sphere–plate geometry shown, given the Hamaker constants, which can be found in the literature for various materials or calculated from optical properties (French 2000) and the separation between the particle and the surface, which is taken as 0.4 nm for smooth surfaces. The contact radius can be calculated using various models of elastic or plastic deformation. The electrostatic forces are more difficult to calculate, requiring knowledge of the surface charge density (Visser 1995), and will dissipate with time. We can neutralize the surface after applying the particles. However, during swiping, charge

transfer can occur due to contact electrification (Lowell and Rose-Innes 1980). Capillary forces can be calculated for a sphere–plate geometry given the surface tension of the liquid, the particle radius and the contact angle (Visser 1995, Busnaina and Elsayy 2000, Xiao and Qian 2000).

### 1.2. Approach

There are many complexities in real swiping experiments that may render the model described by figure 1 inadequate. In contrast to studies of particle removal from smooth, flat semiconductor wafers, our surfaces and traps are very far from the ideal geometry. For example, the types of surfaces sampled in explosive screening environments include the exteriors and interiors of carry-on luggage, laptop computers, cosmetics bags, etc. The traps themselves can be woven cloths or papers of cotton or fiberglass. The particles are likely to be non-spherical, and can be expected to be in a heterogeneous matrix containing the sebaceous materials (body oils) common to latent fingerprints. The complex surface textures change the real contact areas among the particle, surface and trap, changing the adhesion forces. Critical to modeling the contact area is the size and distribution of surface asperities while under compression (Cooper *et al* 2001, Burdick *et al* 2001), which in our case would have to be determined for both trap/particle and particle/surface interactions under an applied load. Such a measurement presents significant challenges. It is possible to calculate van der Waals forces for particles in media other than air or vacuum (Visser 1995, French 2000), although the heterogeneous nature of the matrix will make this challenging.

Our experimental approach was designed to gauge the importance of these factors for future modeling efforts and to provide practical information that can be of immediate use, such as the collection efficiency of individual traps and the optimal force to use during swiping. We use surfaces and traps representative of those encountered in a screening environment, even though the textures and chemistries might be difficult to characterize. We chose, for simplicity, to use spherical particles, because of the ability to control the particle size and to simplify particle counting (through use of a fluorescent tag). The particles are deposited in two ways, either dry or in a matrix of sebaceous material, to incorporate some of the real complexity. The frictional force and normal load are controlled and measured using a device that provides reproducible swiping. The particle collection efficiency is determined by measuring the number of particles collected on the trap and left behind on the surface, using an optical microscopy approach.

## 2. Experimental details

### 2.1. Test particles

The particle sizes of the explosives in fingerprints produced from handling C-4 and Semtex H range from 1  $\mu\text{m}$  or smaller to larger than 50  $\mu\text{m}$  (Verkouteren 2007). The particles 10  $\mu\text{m}$  and larger are the most critical to target for improved detection, and so we selected two particle sizes at approximately 10  $\mu\text{m}$

and 40  $\mu\text{m}$ . Two samples of fluorescent polystyrene latex (PSL) spheres were purchased in an aqueous solution (Polysciences Inc., Warrington, PA<sup>1</sup>) with diameters of  $9.00 \pm 1.3 \mu\text{m}$  and  $42 \pm 6.7 \mu\text{m}$ , as reported by the manufacturer. The spheres are fluorescent to aid in the optical imaging described later.

Aliquots of the spheres in the solution were diluted and filtered onto polycarbonate filters. Any charging of the filters was neutralized by suspending a polonium strip approximately 1 cm above the surface. Efforts were made to produce filters with uniform, unagglomerated particles, since clusters of particles complicate the counting procedures. The particles were transferred to the test surfaces in two ways: either dry or by mixing the particles with a sebaceous material and transferring the mixture to the surface as a fingerprint. The artificial sebum was prepared by following the procedure outlined in ASTM (1997), and contains the following: palmitic, stearic, oleic and linoleic acids, coconut oil, paraffin wax, olive oil, squalene and cholesterol. (Latent fingerprints also contain eccrine sweat components that were not included in the preparation.) The sebum was massaged onto a gloved finger, and then the particle filter was touched and a fingerprint was made on the test surface. The dry transfer was accomplished by lightly brushing the surface of the filter to the test surface. The dry transfer represents a gentle deposition, producing the smallest contact area (Rimai *et al* 1990). The particles were contained within a 2.5 cm  $\times$  2.5 cm area on the test surfaces, and any electrostatic charging developed during particle transfer was neutralized by suspending a polonium strip above the surface.

### 2.2. Test surfaces

Four test surfaces were selected to represent some of the target surfaces at screening venues in airports. These include (1) textured vinyl, (2) smooth vinyl, (3) a stiff cotton fabric and (4) a thin nylon fabric (figure 2). All four materials were purchased in large quantities at a fabric store (Jo-Ann Fabric and Crafts Store, Gaithersburg, MD) and then cut into 23 cm  $\times$  8.5 cm pieces.

Surface roughness measurements were made over a 0.64 mm<sup>2</sup> area with a NanoFocus  $\mu\text{surf}$  3D confocal surface measurement system (NanoFocus Inc., Glen Allen, Virginia). The results are given in table 1 as the average surface roughness  $S_a$  and the root mean square (rms) roughness  $S_q$ , and represent overall measures of the textures comprising the surfaces. Both measures of roughness are generally insensitive to peaks and valleys, such as the features seen on the textured vinyl surface in figure 2. Problems were encountered in the measurement of the fabrics because of extreme height differences arising both from fibers extending off the surface and from the holes in the weave. Both of these problems caused the measurements at some locations in the sampled area to exceed the measurement range.

<sup>1</sup> Certain commercial equipment, instruments or materials are identified in this document. Such identification does not imply recommendation or endorsement by the National Institute of Standards and Technology, nor does it imply that the products identified are necessarily the best available for the purpose.

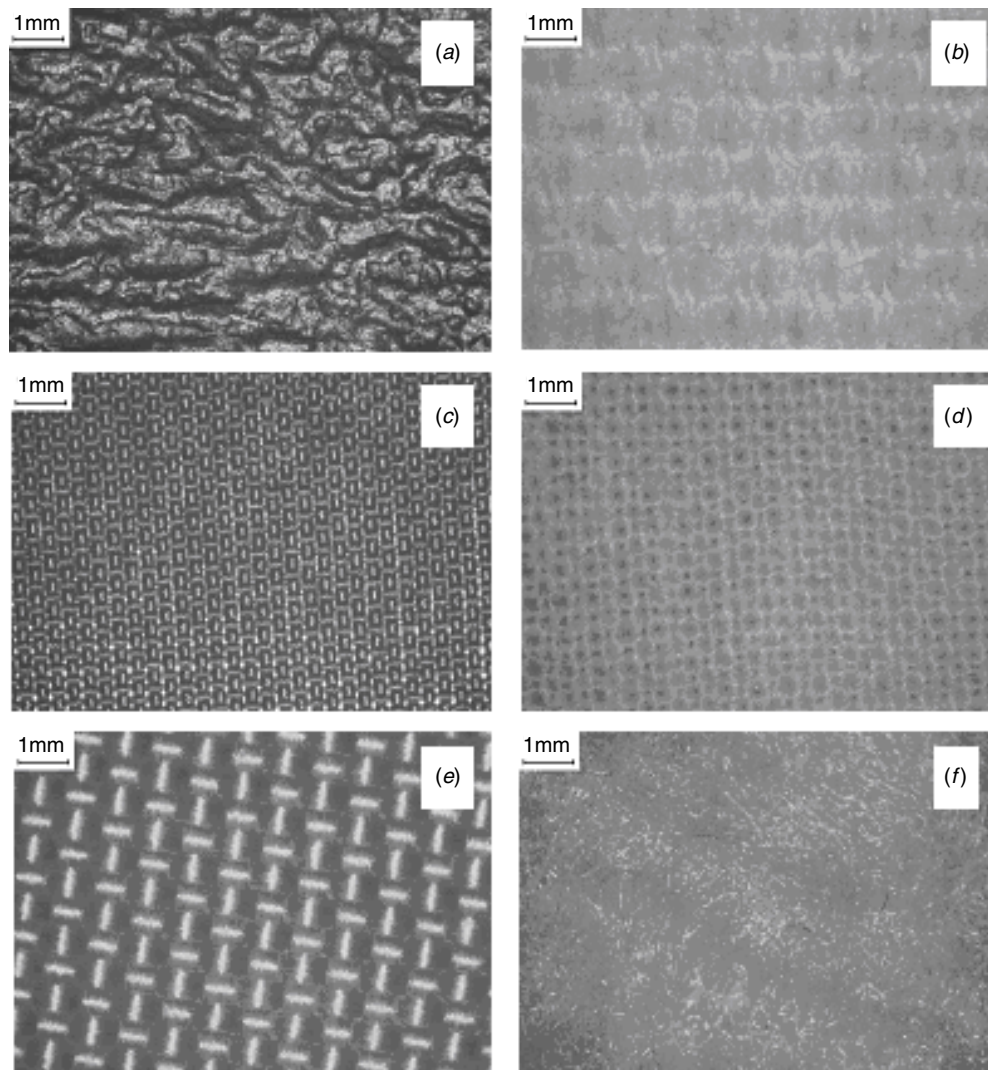


**Figure 2.** Micrographs of test surfaces (a)–(c) and sample traps (d)–(f). (a) Textured vinyl, (b) cotton fabric, (c) nylon fabric, (d) muslin, (e) PTFE and (f) Swiffer. The smooth vinyl material is transparent and therefore the surface is difficult to image; a micrograph is not included.

**Table 1.** Roughness values for test surfaces and traps.

Surface or trap	Average roughness ( $\mu\text{m}$ )	Rms roughness ( $\mu\text{m}$ )
Vinyl (textured)	3.3	3.9
Vinyl (smooth)	0.1	0.2
Cotton fabric	48.3	55.3
Nylon fabric	8.7	11.2
Muslin trap	95.8	115.8
PTFE trap	5.7	7.5

### 2.3. Sample traps

Two different sample traps were used in the experiments, both of which are sold for use with IMS instruments. These include a woven, cotton cloth (muslin) and a proprietary polytetrafluoroethylene (PTFE, also known as Teflon)-coated woven fiberglass trap. The surface roughness of the two traps was measured as described earlier for the test surfaces, and the results are given in table 1.

In addition, a limited number of experiments were conducted with a cloth sold commercially for household dust collection (Swiffer Sweeper dry cloths, Proctor & Gamble). The Swiffer dry cloth has a patented texture and surface treatment designed to enhance particle collection. The texture is a non-woven, hydroentangled texture (Fereshtekhou *et al* 2004), produced by using water jets to entangle fibers and form a cloth. The composition of the cloth is not specified. The Swiffer dry cloth cannot withstand the desorber temperatures of commercial IMS instruments, but was included as an example of a material designed specifically for particle collection. The two sample traps and the dry cloth are shown in figures 2(d)–(f) to illustrate their textures.

### 2.4. Swiping

The critical factors to control and/or measure during swiping are the load and the frictional force. For this purpose, we use a slip/peel instrument (IMASS Inc., Accord, MA), which provides for reproducible swiping and measurement of the

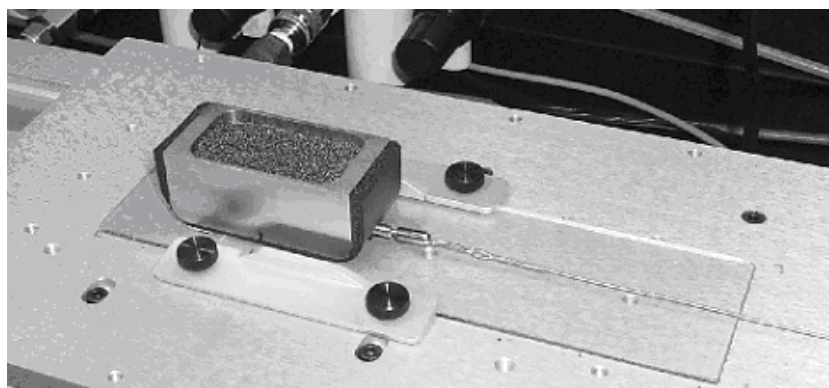


**Figure 3.** The slip/peel instrument used for reproducible swiping. The sled, filled with lead shot, sits on a glass slide on the translatable platen and is held in place with a guide wire.

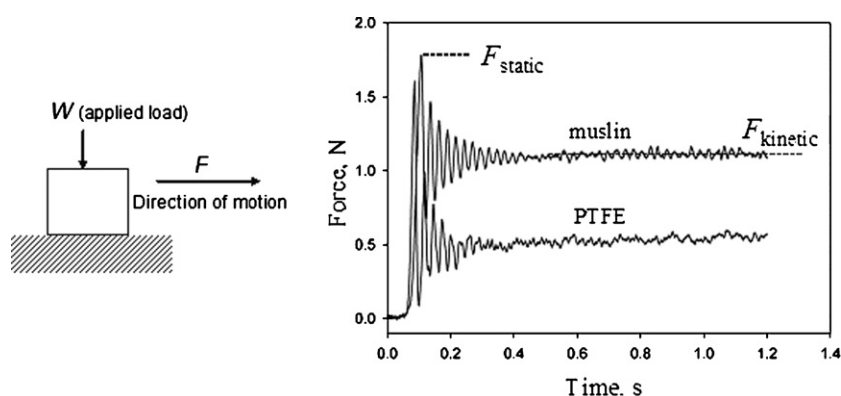


**Figure 4.** Schematic illustration of sled sliding with respect to a surface where  $W$  is the applied load and  $F$  is the tangential force, and actual trace of  $F$  versus time for both traps on the textured vinyl using the light weight.

frictional force. This type of instrument is used in the textile industry to test the transfer of dye from a fabric during rubbing, and is also widely used to test adhesion. It has a sled that sits on a platen that can be programmed to move a set distance at a known velocity (figure 3). The sample trap is placed on the bottom of the sled, and the surface containing the particles of interest is placed on the platen. The platen is then translated, moving the test surface below the stationary sample trap. The tangential forces generated during sliding are shown schematically in figure 4, along with the measurements recorded for two experiments. The response is typical for this type of experiment, with a higher static force required to initiate sliding and a lower kinetic force required to maintain sliding (Bhushan 2003).

The load on the surface can be controlled by the simple addition of weights to the sled. Two different sled weights were used, a light weight of 325 g and a heavy weight of 1275 g. The light weight is not based on any expected swiping force, but resulted simply from filling the basin in the sled to the top with lead shot. The heavy weight represents an estimate of the force required for a firm pressure during swiping. To arrive at this estimate, ten people from our laboratory were given a wand with an attached sample trap and were asked to swipe with the 'firm' pressure. The wand is sold for use with a commercial IMS instrument and is used to hold traps during swiping. The swiping was conducted on a pressure-sensitive

surface (Tekscan Inc., South Boston, MA). There was a large range in the normal force used, from a minimum of 1000 g to a maximum of 2300 g, and we chose a force of 1275 g simply on the basis of available weights. The surface area of the wand/trap combination is much smaller than that of the sled (3.9 cm<sup>2</sup> compared with 15.2 cm<sup>2</sup>), and therefore the pressure distribution will be different between the two swiping methods, but the goal was to approximate a reasonable normal force. The bottom of the sled is not completely flat, with the result that the pressure is lower in the center (figure 5). It is common in tests conducted with hand-held swiping to see contact areas that show uneven distributions in pressure or that change in the total area during swiping. The advantage of the sled and the slip/peel instrument is that the contact area is reproducible for all experiments, even if the pressure distribution is not ideal.

To conduct the swiping experiments, the sled with an attached sample trap was placed directly onto the 2.5 cm × 2.5 cm area containing the test particles. The muslin trap fully covered the bottom of the sled, but the PTFE trap is 2.6 cm wide and therefore narrower than the sled. The platen was translated at a rate of 0.7 cm s<sup>-1</sup> immediately upon placement to avoid adhesion of the sled to the surface. The traverse distance of the platen was initially set to 4.2 cm, but was reduced to approximately 2 cm in order to limit the area over which the particles needed to be counted.

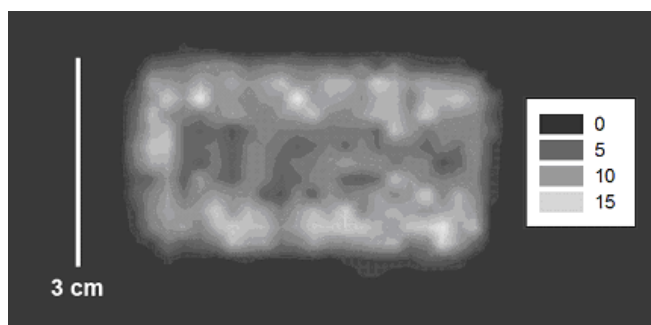


**Figure 5.** Pressure in kPa over the surface of the sled with the heavy weight attached. Measurements conducted on the pressure-sensitive surface (Tekscan, Inc.).

### 2.5. Environmental conditions

All experiments were conducted in the Advanced Measurement Laboratory at NIST under controlled conditions of relative humidity ( $45\% \pm 5\%$ ). The samples were swiped within 8 h following deposition of the particles, as ageing is known to increase adhesion. Tang and Busnaina (2000) found that ageing-induced adhesion occurred only at high humidity for  $22\ \mu\text{m}$  PSL spheres on silicon. At relative humidities of 45% or less, the adhesion did not change significantly within 24 h. Busnaina and Elsayy (2000) determined that the capillary force dominates the adhesive force only at relative humidities above 70% for PSL on a variety of substrates, and that electrostatic forces dominate below 45% RH. Grobely *et al* (2006), on the other hand, found that the capillary force is the dominant adhesive force in ambient air, and that it persists even at  $<1\%$  RH (in a nitrogen atmosphere).

### 2.6. Measurement of collection efficiency

A common approach to measuring particle removal from surfaces is to define an area on the substrate and compare particle counts from that area before and after particle removal. The defined area is typically a small fraction of the particle deposit. To determine collection efficiencies, we need to count the entire particle deposit, before and after swiping, and count the particles transferred to the sample trap. The particle deposits were confined to a  $2.5\ \text{cm} \times 4.5\ \text{cm}$  area (adding the 2 cm travel distance to the starting dimensions), but these areas were still too large to be contained within a single image at the magnifications required to reliably count the spheres. To cover the entire area, we collected a tiled image, which is a mosaic of smaller, contiguous images. Tiling has the advantage of producing a complete image of the deposit, including the movements of individual particles.

To create a tiled image, an automated stage is required that can accurately advance the exact distance corresponding to the dimensions of an image. This requires mechanical accuracy in the stage, an accurate calibration of the magnification and an exact alignment of camera and stage. An automated Prior ProScan X-Y-Z sample stage (Prior Scientific Inc., Rockland, MA) with a repeatability of  $\pm 1\ \mu\text{m}$  was used for this purpose. The stage was attached to a Zeiss M2Bio fluorescent microscope system (Carl Zeiss MicroImaging Inc., Thornwood, NY), and images were collected in a fluorescence

mode with an Evolution MP digital CCD non-cooled color camera (Media Cybernetics Inc., Silver Spring, MD). Images were collected as 12-bit gray level images with a resolution of  $1280 \times 960$  pixels. The tiled images were composed of approximately eight smaller images for the  $42\ \mu\text{m}$  spheres and 210 smaller images for the  $9\ \mu\text{m}$  spheres. Magnification calibration was accomplished through use of a calibration slide provided by Media Cybernetics, and then tested using a microscopy size standard produced by Geller Microanalytical Laboratory (Topsfield, MA) and traceable to NIST. Control over the automation, including stage movement and image collection, was accomplished through the software program ImagePro (Media Cybernetics Inc.). The particle count was determined by image analysis with ImagePro, using an automated bright particle threshold.

The quality of the tiling procedure can be evaluated by imaging a regular array of features, such as the array of nominal  $100\ \mu\text{m}$  fluorescent spots, shown in figure 6. The image was collected at  $20\times$  magnification, which is one of the magnifications used to image the  $42\ \mu\text{m}$  spheres. Small errors in alignment are observed in the top row and left column of spots, and the spot in the top-left corner shows errors arising from the intersection of four images. The errors in alignment are on the order of  $\pm 5\ \mu\text{m}$ , which is approximately equal to the resolution in the magnification calibration ( $3.3\ \mu\text{m}/\text{pixel}$ ). The magnification used primarily to image the  $9\ \mu\text{m}$  spheres is  $80\times$ , which has an image resolution of  $1.0\ \mu\text{m}/\text{pixel}$ .

There is the possibility that errors in image alignment during tiling can result in the loss or addition of counted particles, particularly for the smaller spheres. The ability to obtain an accurate count of particles that are aggregated into clusters is of larger concern. Clusters of particles were observed, both before and after swiping, and were analyzed to determine individual particle counts. The area of each thresholded particle was used as an initial step in separating single particles from clusters. Because there is variability in the size of the particles, the area could not be used to reliably determine the number of particles in a cluster. A software feature allows the generation of a 'sorted object image', which sorts the thresholded objects according to any measured value, in this case area. A corrected total particle count was achieved by direct observation of the clusters and assignment of a particle number to each cluster (figure 7). Any particle that is not spherical due to image alignment problems can also

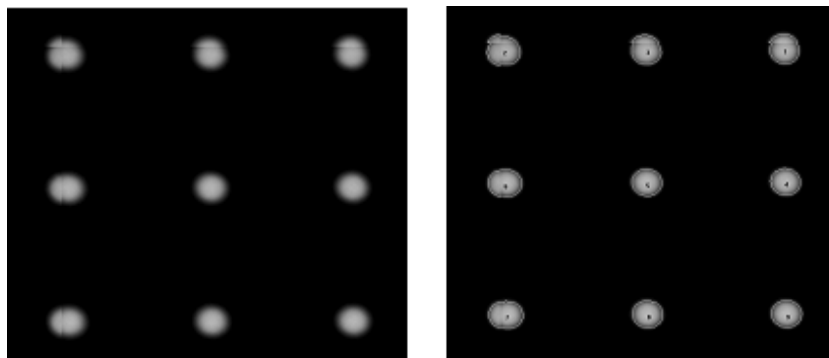


**Figure 6.** The portion of the tiled image of a fluorescent array of nominal  $100\ \mu\text{m}$  spots showing slight errors in image alignment. Image as collected (left) and thresholded using a bright particle threshold (right).



**Figure 7.** Examples of clusters of  $9\ \mu\text{m}$  spheres from a representative image. Sphere numbers assigned to clusters are, from left, 8, 5, 3, 2, 3, 2, 3, 2, 2, 2, 2, 2, 2, 2.

be observed. Because the counting errors are operating in a random fashion, their magnitude can be evaluated from the recovery rate, which is the ratio of the particles found after swiping (on the surface and on the sample trap) to the starting number. For a measurement process under control, the recovery rate should average 100%.

### 3. Results

#### 3.1. Method validation

The recovery rates of the particles after swiping are summarized in table 2. The averages are presented with respect to the two particle sizes, and include the data from all surfaces and from both methods of deposition. The recovery rates are not significantly different from 100%, which shows good control on the counting errors. Initially, we planned to use both methods of deposition on all four surfaces, but observed a low recovery rate of approximately 60% for the dry-deposited  $42\ \mu\text{m}$  particles on the nylon fabric. We suspected that the particles might be lost due to gravitational effects from handling the surface following particle deposition. The  $42\ \mu\text{m}$  particles were dry-deposited on all four surfaces, and the surfaces were agitated. There was loss of particles from the nylon fabric, but not from the remaining surfaces. For the nylon fabric, we decided to use only the sebum deposition method for both particle sizes and dispense with the dry deposition method.

The tangential forces recorded by the slip/peel instrument during swiping were evaluated for all combinations of the trap, surface and normal force, and were repeated five times each. The results are given in table 3. Because the PTFE trap did not fully cover the base of the sled, additional trap material was used to fill in the area to avoid contact of the base of the sled with the test surface. Since the tangential force is

**Table 2.** Recovery of particles following swiping. Standard uncertainties ( $s/\sqrt{n}$ ) reported.

Particle diameter ( $\mu\text{m}$ )	Recovery (%)	# of experiments	Particles/experiment
9	$101.4 \pm 2.4$	49	$294 \pm 57$
42	$98.5 \pm 2.1$	51	$107 \pm 11$

averaged over the entire active surface, this was the only way to evaluate the forces due solely to the interaction of the PTFE trap with the various surfaces. The results indicate that there is no correlation between the roughness of the surface, as given in table 1, and the tangential forces recorded during swiping. There are many physical and chemical properties of the surfaces that can affect adhesion and sliding. Surface roughness is only one factor, and can actually serve to decrease frictional forces by reducing the contact area.

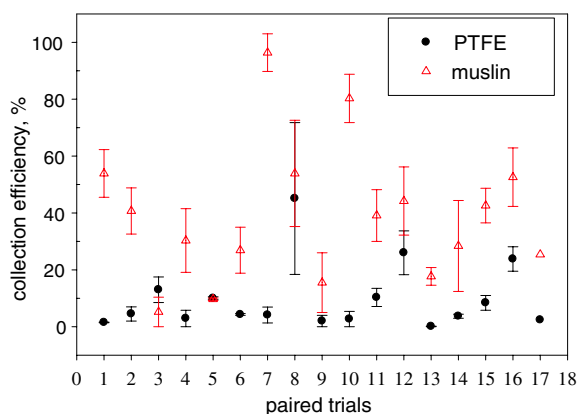
The nylon fabric surface is different from the other three surfaces, with consistently lower tangential forces. This indicates lower adhesion of the traps to that particular surface; lower adhesion of the particles to the nylon surface is also indicated by the loss of dry particles after deposition, as described earlier. There is also a difference between the traps with a smaller force generated by the PTFE trap on each surface as compared with the muslin trap. The increase in the tangential force scales approximately with the normal force, with an increase of 3–5 times for an increase in the applied load of four times.

#### 3.2. Collection efficiencies

The collection efficiencies determined from the swiping experiments are given in tables 4–7. Collection efficiency was calculated as the number of particles found on the sample trap relative to the number initially measured on the test surface

**Table 3.** Tangential forces measured during swiping. Standard uncertainties reported.

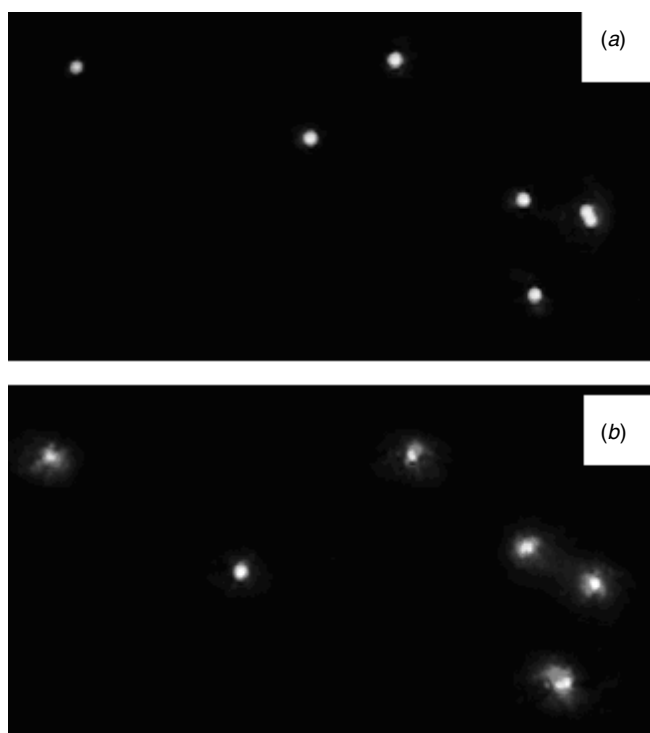
Surface	$F_{\text{kinetic}}$ (N)			
	325 g		1275 g	
	PTFE	Muslin	PTFE	Muslin
Vinyl (textured)	$0.53 \pm 0.0002$	$0.94 \pm 0.0010$	$2.73 \pm 0.0006$	$4.25 \pm 0.0006$
Vinyl (smooth)	$0.58 \pm 0.0002$	$1.11 \pm 0.0005$	$2.91 \pm 0.0010$	$3.55 \pm 0.0010$
Cotton fabric	$0.67 \pm 0.0010$	$1.16 \pm 0.0010$	$2.45 \pm 0.0010$	$4.50 \pm 0.0040$
Nylon fabric	$0.38 \pm 0.0007$	$0.74 \pm 0.0002$	$2.07 \pm 0.0007$	$3.13 \pm 0.0009$

**Figure 8.** Comparison of collection efficiencies for PTFE versus muslin traps. Bars represent standard uncertainties.

being swiped. Multiple trials ( $n = 2-6$ ) were conducted for experiments using the light weight, and the mean and standard uncertainty are presented. A more limited number of experiments were conducted using the heavy weight.

One conclusion from the data is that there is a difference in collection efficiency between the two sample traps. In 14 of 17 direct comparisons of the two traps, the muslin trap had significantly higher collection efficiencies than the PTFE trap (figure 8). For some conditions, close to 100% collection efficiencies are observed for the muslin trap, whereas the highest collection efficiency for PTFE is 45%, and these results exhibit a high variability. The average collection efficiency for the PTFE trap is 10%, whereas the average collection efficiency for the muslin trap is 39%. Those particles that were collected by the PTFE trap were often on the leading edge, where some fraying of the fibers occurs, or on a circular opening in the trap that also had rough edges. The muslin trap has fibers extending randomly off the surface, and these were often sites for particle attachment.

Of the four surfaces, there are no clear differences in collection efficiency among the two vinyl surfaces and the nylon fabric, but particles are generally more difficult to collect off of the cotton canvas; this difference is more apparent for the larger particles. The cotton surface is probably difficult to sample because the particles are pushed into the weave of the fabric during swiping (figure 9). Although the nylon fabric also has a woven structure, providing holes for the particles, it has a smoother surface texture and the particles can move more easily, as evidenced by the loss of the dry-deposited particles by simple agitation. The presence of surface topography

**Figure 9.**  $42 \mu\text{m}$  particles on the cotton canvas before (a) and after (b) swiping. Particle outlines are fuzzy in (b) because the particles are below the surface of the fabric. The surface of the trap is in focus for both images, although not visible in the images.

does not decrease collection efficiencies, as the textured vinyl surface has some of the highest collection efficiencies among the surfaces.

The heavy weight does not greatly improve collection efficiency. In seven of ten direct comparisons, the heavy weight produces higher collection efficiencies, but with relatively modest gains (figure 10). In only one case, there is an improvement higher than 25% (for the sebum-deposited  $42 \mu\text{m}$  spheres on smooth vinyl). The average collection efficiency for the light weight is 25%, compared with 35% for the heavy weight. The absence of a large improvement was unexpected, as the heavy weight is four times that of the lighter. The normal force represented by the light weight would be viewed by most as a light touch on the surface.

When considering the results for the muslin sample trap only, the collection efficiency is marginally higher for the larger particles compared with the smaller particles (six/nine direct comparisons) and for the sebum-deposited particles compared with the dry-deposited particles (five/eight direct

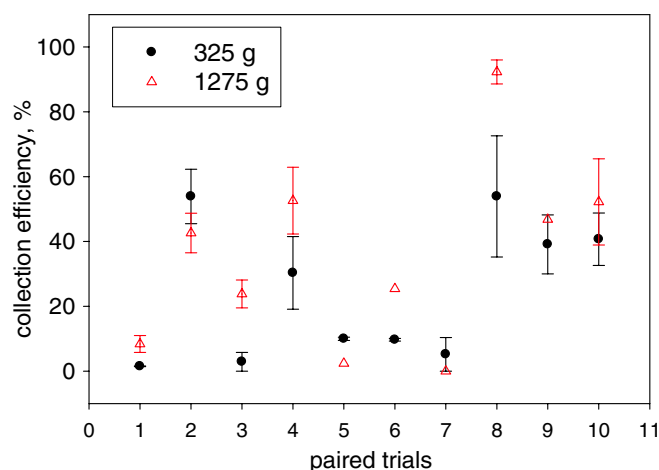


**Figure 10.** Comparison of collection efficiencies for light versus heavy weight.

comparisons). These differences are more apparent if the cotton canvas surface is disregarded (six/seven and five/six comparisons, respectively). In studies of particle removal from surfaces, a general reduction in removal efficiencies with the decreasing particle size has been reported, and is ascribed to differences in the rate of change in adhesive and removal forces with respect to the particle size (Ranade 1987, Xu *et al* 2005).

The lowest collection efficiency (0%) is observed for the cotton surface with the muslin trap and heavy weight, the same combination that has the highest sliding force. Although there are problems with the particles being pushed into the cotton fabric, it is clear that the application of more force to detach particles is not the only, or even the most important, consideration for collection efficiency. We consistently see movement of particles following swiping, as indicated by the relative positions of particles before and after swiping (figure 11). Quantitative measures of particle movement were not attempted for this study, but we observed some movement on all surfaces, with both light and heavy weights and with both types of sample traps.

#### 4. Discussion

The fact that we see movement of the particles (either through rolling or sliding) indicates that sufficient force is present to overcome the adhesion moments for many of the particles. After the particles are detached, there should be a much lower force required for lifting. Increasing the frictional force does not result in a great improvement in collection efficiency, which indicates that improvements must come from better adhesion to the sample trap. The Swiffer dry cloth has characteristics that result in improved particle adhesion, as demonstrated by the results given in table 8. With the Swiffer we see a 100% collection efficiency for the dry-deposited 42  $\mu\text{m}$  spheres, compared with a 43% collection efficiency for the muslin trap under the same conditions. The 73% collection efficiency for the Swiffer on the cotton canvas is even more striking, given that the highest collection efficiency

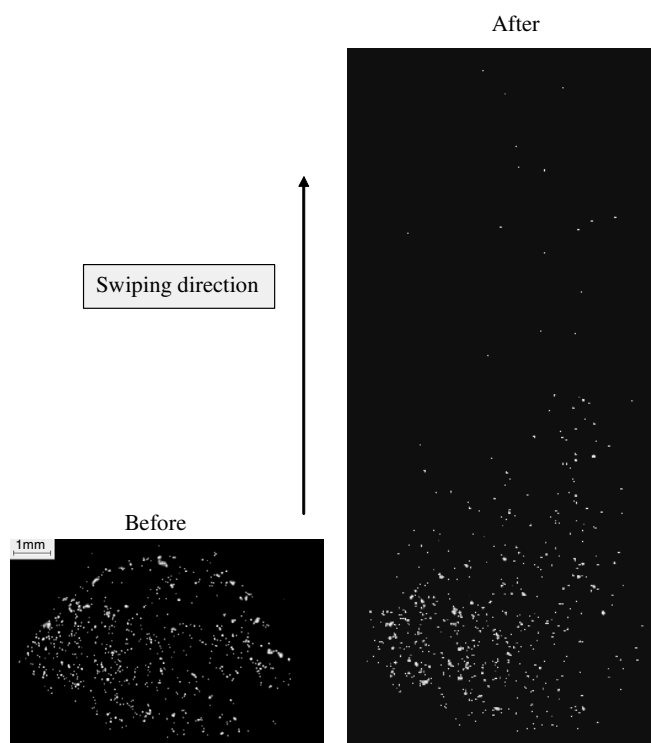


**Figure 11.** 9  $\mu\text{m}$  sebum-deposited spheres on textured vinyl, swiped with muslin. Movement of spheres is apparent after swiping.

for that surface using the other two sample traps is 27%. Even more compelling is the fact that the particles can be collected without using any frictional force, as given by the results labeled ‘applied load only’ in table 8. With the heavy weight attached, 84% of the 42  $\mu\text{m}$  particles are collected and 27% of 9  $\mu\text{m}$  particles are collected. By comparison, hardly any particles are collected with the applied load only using the muslin sample trap.

In evaluating the reasons why the Swiffer would have such improved collection efficiencies, we must consider both the composition and the texture. The Swiffer patent states a number of possible compositions, including fibers of polyester, polypropylene, nylon or a similar polymer, and there may be a surface coating of wax or mineral oil. We are currently attempting to obtain samples of Swiffer cloths with identified chemistries and without any surface coatings. The texture is quite distinctive, particularly when compared with the two IMS traps, as shown by the cross sections shown in figure 12. The two IMS traps are both woven (the sinuous patterns in figure 12), whereas the Swiffer has a looser, more chaotic structure. It is possible that the looser structure of the Swiffer presents multiple sites of attachment for a single particle, which would increase the van der Waals force. A theoretical model of dispersion forces for particles with respect to infinite cylinders (fibers) has been developed (Montgomery *et al* 2000), but for one site of attachment only. The authors caution that the complexity introduced by different geometries results in a model that should be used only to provide estimates of the forces. Therefore, models for multiple sites of attachment will probably not be feasible at this time.

**Table 4.** Collection efficiency of dry-deposited 42  $\mu\text{m}$  PSL spheres.

Surface	Collection efficiency (%)			
	325 g		1275 g	
	PTFE	Muslin	PTFE	Muslin
Vinyl (textured)	1.5 $\pm$ 1.1	53.9 $\pm$ 8.4	8.4 $\pm$ 2.6	42.6 $\pm$ 6.1
Vinyl (smooth)	4.5 $\pm$ 2.5	40.7 $\pm$ 8.1		52.2 $\pm$ 13.3
Cotton fabric	13.0 $\pm$ 4.5	5.2 $\pm$ 5.2		0

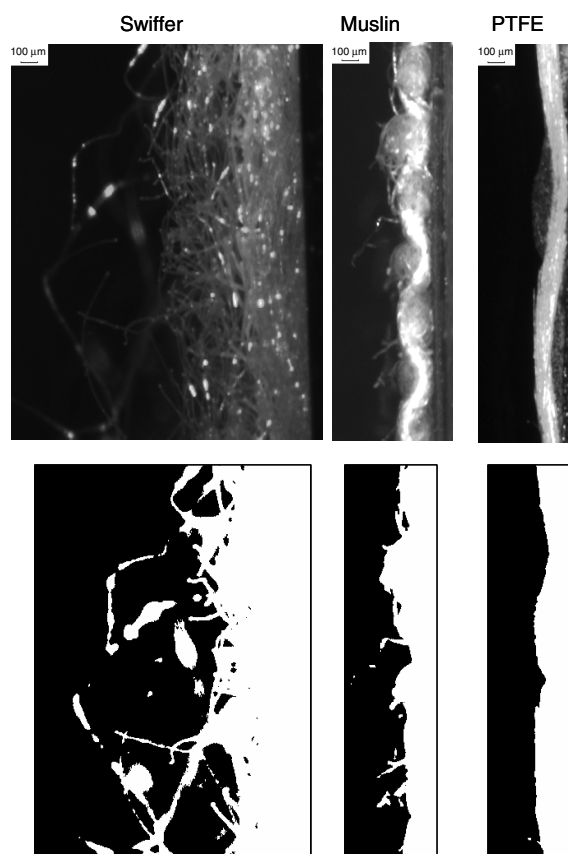
**Table 5.** Collection efficiency of dry-deposited 9  $\mu\text{m}$  PSL spheres.

Surface	Collection efficiency (%)			
	325 g		1275 g	
	PTFE	Muslin	PTFE	Muslin
Vinyl (textured)	2.9 $\pm$ 2.9	30.3 $\pm$ 11.2	23.8 $\pm$ 4.3	52.6 $\pm$ 10.3
Vinyl (smooth)	10.0 $\pm$ 0.5	9.7 $\pm$ 0.4	2.4	25.4
Cotton fabric	4.3 $\pm$ 0.3	26.9 $\pm$ 8.1		

It may be enough to have a measurement approach to describe the texture, particularly the texture on the scale of the particle, in order to compare the effectiveness of different traps. One approach we are investigating is that proposed by Steele *et al* (2006) to use digital imaging to evaluate the textile surface roughness. Optical images are collected and thresholded, as shown in figure 12. The low frequency roughness introduced by macroscopic texture, such as the sinuous profile of the PTFE trap, can be modeled and removed to evaluate the high frequency roughness (Steele *et al* 2006). A more interesting measure might be the surface contact area, calculated with respect to different particle sizes, although it would be the contact area for an uncompressed geometry. Evaluating the expected contact area between particles of different sizes and the surface might provide an explanation of the differences in collection efficiency with respect to the particle size.

The texture of the test surface does not seem to be a critical factor, as the collection efficiencies are not strongly correlated with the surface, with the exception of the cotton fabric. This is probably due to the fact that we have sufficient force to remove the particles from the surfaces, as we see particle movement on all the surfaces (even the cotton fabric). Surfaces that will allow embedding of the particles, such as the cotton fabric, should be avoided in sampling, unless an IMS trap can be developed that allows particle collection with no frictional forces.

Both texture and composition may contribute to the poor collection efficiencies of the PTFE trap. It is not unreasonable that this material was chosen as a trap material, as it had been demonstrated to be appropriate for thermal desorption of explosives (Sigman and Ma 1999). Sigman and Ma used PTFE tubing as a dry surface wipe, and they abraded the surface to enhance surface contact. However, they were primarily concerned with desorption characteristics, rather than collection efficiencies. The texture of the trap is very smooth, compared with the muslin trap and the Swiffer. We did not abrade the trap, as that would have exposed the underlying

**Figure 12.** Cross-sectional optical microscope images of traps as collected (top) and thresholded (bottom). The scale bars in the images are 100  $\mu\text{m}$  in size.

fiberglass, changing the composition along with the texture. PTFE was designed as a nonstick material, and the van der Waals forces for particles with respect to this surface are low. In some cases, the van der Waals interactions for PTFE are repulsive, which is the definition of nonstick (Drummond and

**Table 6.** Collection efficiency of sebum-deposited 42  $\mu\text{m}$  PSL spheres.

Surface	Collection efficiency (%)			
	325 g		1275 g	
	PTFE	Muslin	PTFE	Muslin
Vinyl (textured)	4.1 $\pm$ 2.8	96.4 $\pm$ 6.6		
Vinyl (smooth)	45.1 $\pm$ 26.7	53.9 $\pm$ 18.7		92.3 $\pm$ 3.7
Cotton fabric	2.0 $\pm$ 2.0	15.5 $\pm$ 10.5		
Nylon fabric	2.7 $\pm$ 2.7	80.3 $\pm$ 8.5		

**Table 7.** Collection efficiency of sebum-deposited 9  $\mu\text{m}$  PSL spheres.

Surface	Collection efficiency (%)			
	325 g		1275 g	
	PTFE	Muslin	PTFE	Muslin
Vinyl (textured)	10.3 $\pm$ 3.2	39.1 $\pm$ 9.1		46.8
Vinyl (smooth)	26.0 $\pm$ 7.7	44.2 $\pm$ 12.0		
Cotton fabric	0.1 $\pm$ 0.1	17.7 $\pm$ 3.1		
Nylon fabric	3.7 $\pm$ 0.7	28.4 $\pm$ 16.0		

**Table 8.** Collection efficiency of dry-deposited PSL spheres with heavy weight, comparing Swiffer dry cloth to muslin.

Trap	Surface	Collection efficiency (%)		
		42 $\mu\text{m}$	42 $\mu\text{m}$ , applied load only	9 $\mu\text{m}$ , applied load only
Swiffer	Vinyl (textured)	100	84.0 $\pm$ 7.1	26.9
Swiffer	Cotton fabric	73.1		
Muslin	Vinyl (textured)	42.6 $\pm$ 6.1 <sup>a</sup>	2.2	
Muslin	Cotton fabric	0 <sup>a</sup>		

<sup>a</sup> From table 4.

Chan 1996). Geckos are marvels in the animal world in being able to stick to almost every surface, but even they cannot stick to PTFE (Autumn 2006). It is also difficult to adhere particles to PTFE through capillary forces because of the nonpolar nature of PTFE. In addition to van der Waals and capillary forces, the electrostatic forces are influenced by composition. When two surfaces are rubbed together, the transfer of charge results in one surface being positively charged while the other is negatively charged. Triboelectric series have been developed that rank in order the relative propensity for surfaces to adopt either a positive or a negative charge, and PTFE is highly weighted to the negative side (Lowell and Rose-Innes 1980). Cotton (i.e. muslin), on the other hand, tends to develop a positive charge. Future experiments will involve the measurement of surface charge in order to evaluate the charges on the surface, trap and particle during swiping.

It is not immediately obvious why the particles embedded in the sebum are more efficiently collected than the dry particles. The improvements in collection efficiencies are observed for the muslin trap only, and not for the PTFE trap. The artificial sebum is a sticky material, and therefore adheres to surfaces due to increased surface contact. We do not know at this time why it would preferentially adhere to the trap, rather than the test surface. We did not carefully

control the ratio of sebum to the particle, and the particles could be either completely embedded in the sebum or simply coated by the sebum. We also need to investigate the effects of ageing on collection efficiencies. Latent fingerprints are known to change the composition with time, with loss of the unsaturated lipids (e.g. squalene and oleic acid), although the saturated compounds such as palmitic and stearic acids remain unchanged (Ramotowski 2001).

## 5. Conclusions

This study was designed to provide an experimental approach to determine particle collection efficiency during swipe sampling. We have demonstrated a significant difference in the collection efficiency of two sample traps for PSL spheres, either dry or in sebaceous material. The particular PTFE trap investigated here has a fairly poor collection efficiency that is independent of the surface type, applied load or particle size. Muslin traps can exhibit fairly high collection efficiencies from some surfaces, but collection off of a heavy cotton fabric, a material that forms the outside of many soft suitcases, is very difficult. Muslin has the highest collection efficiencies for large (42  $\mu\text{m}$  diameter) particles, particularly those contained in a sebaceous matrix. Finally, the more downward applied

force, as represented by our heavy sled weight, does not necessarily improve collection efficiencies.

We plan to continue our investigations to develop a modeling approach for prediction of collection efficiencies for different traps. Our experimental design provides for the determination of the frictional forces acting on the particles and the calculation of the particle collection efficiency. The adhesion and removal forces can be calculated using an ideal geometry, but we have demonstrated that the texture of the trap must be considered. Commercial developments of dust collection traps may point to ways to improve particle collection efficiencies, as indicated by the results for the Swiffer dry cloth. Although IMS detection has additional requirements for sample traps in terms of thermal stability and low volatile background, the approaches to texture modification might be useful to explore.

## Acknowledgments

Surface roughness measurements were performed by Alan Zheng in the NIST Manufacturing and Engineering Laboratory. The Department of Homeland Security sponsored the production of this material under an Interagency Agreement with the National Institute of Standards and Technology.

## References

- ASTM 1997 Standard guide for evaluating cleaning performance of ceramic tile cleansers *Annual Book of ASTM Standards, Technical Report ASTM D 5343-97*
- Autumn K 2006 How gecko toes stick *Am. Sci.* **94** 124–32
- Bhushan B 2003 Adhesion and stiction: mechanisms, measurement techniques and methods for reduction *J. Vac. Sci. Technol. B* **21** 2262–96
- Burdick G M, Berman N S and Beaudoin S P 2001 Describing hydrodynamic particle removal from surfaces using the particle Reynolds number *J. Nano. Res.* **3** 455–67
- Busnaina A and Elsayy T 2000 The effect of relative humidity on particle adhesion and removal *J. Adhes.* **74** 391–409
- Cooper K, Gupta A and Beaudoin S 2001 Simulation of adhesion of particles to surfaces *J. Colloid Interface Sci.* **234** 284–92
- Donohue D L 1998 Strengthening IAEA safeguards through environmental sampling and analysis *J. Alloys Compd.* **271–273** 11–8
- Drummond C and Chan D 1996 Theoretical analysis of the soiling of 'nonstick' organic materials *Langmuir* **12** 3356–9
- Eiceman G A and Stone J A 2004 Ion mobility spectrometers in national defense *Anal. Chem.* **76** 390A–397A
- Fereshetkhov S, Russo P J, Strickland W C Jr and Policicchio N J 2004 Three dimensional structures useful as cleaning sheets *US Patent 6797357*
- French R H 2000 Origins and application of London dispersion forces and Hamaker constants in ceramics *J. Am. Ceram. Soc.* **83** 2117–46
- Gresham G L, Davies J P, Goodrich L D, Blackwood L G, Liu B Y H, Thimsem D, Yoo S H and Hallowell S F 1994 Development of particle standards for testing detection systems: mass of RDX and particle size distribution of composition 4 residues *Proc. SPIE* **2276** 34–44
- Grobelyny J, Pradeep N, Kim D-I and Ying Z C 2006 Quantification of the meniscus effect in adhesion force measurements *Appl. Phys. Lett.* **88** 091906
- Hallowell S F 2001 Screening people for illicit substances: a survey of current portal technology *Talanta* **54** 447–58
- Jung H, Kunze J F and Nurrenbern J D 2001 Consistency and efficiency of standard swipe procedures taken on slightly radioactive contaminated metal surfaces *Health Phys.* **80** S80–8
- Lowell J and Rose-Innes A C 1980 Contact electrification *Adv. Phys.* **29** 947–1023
- Montgomery S W, Franchek M A and Goldschmidt V W 2000 Analytical dispersion force calculations for nontraditional geometries *J. Colloid Interface Sci.* **227** 567–84
- Patrick J C and Poziomek E J 1997 Advancement of contraband drug detection through improved surface-sampling procedures *Proc. SPIE* **2937** 130–5
- Ramotowski R S 2001 Composition of latent print residue *Advances in Fingerprint Technology* 2nd edn ed H C Lee and R E Gaensslen (New York: CRC Press) pp 63–104
- Ranade M B 1987 Adhesion and removal of fine particles on surfaces *Aerosol Sci. Technol.* **7** 161–76
- Rimai D S and DeMejo L P 1996 Physical interactions affecting the adhesion of dry particles *Ann. Rev. Mater. Sci.* **26** 21–41
- Rimai D S, DeMejo L P and Bowen R C 1990 Surface-force-induced deformations of monodisperse polystyrene spheres on planar silicon substrates *J. Appl. Phys.* **68** 6234–40
- Sigman M E and Ma C-Y 1999 In-injection port thermal desorption for explosives trace evidence analysis *Anal. Chem.* **71** 4119–24
- Steele C, Jones R and Leaney P G 2006 Tennis ball fuzziness: assessing textile surface roughness using digital imaging *Meas. Sci. Technol.* **17** 1446–55
- Tang J and Busnaina A 2000 The effect of time and humidity on particle adhesion and removal *J. Adhes.* **74** 411–9
- Verkouteren J R 2007 Particle characteristics of trace high explosives: RDX and PETN *J. Forensic Sci.* **52** 335–40
- Visser J 1995 Particle adhesion and removal: a review *Part. Sci. Technol.* **13** 169–96
- Wang H-C 1990 Effects of inceptive motion on particle detachment from surfaces *Aerosol Sci. Technol.* **13** 386–93
- Xiao X and Qian L 2000 Investigation of humidity-dependent capillary force *Langmuir* **16** 8153–8
- Xu K, Vos R, Vereecke G, Doumen G, Fyen W, Mertens P W, Heyns M M, Vinckier C and Fransaeer J 2004 Particle adhesion and removal mechanisms during brush scrubber cleaning *J. Vac. Sci. Technol. B* **22** 2844–52
- Xu K, Vos R, Vereecke G, Doumen G, Fyen W, Mertens P W, Heyns M M, Vinckier C, Fransaeer J and Kovacs F 2005 Fundamental study of the removal mechanisms of nano-sized particles using brush scrubber cleaning *J. Vac. Sci. Technol. B* **23** 2160–75